

Review

Formation of the Outer Shell Layer in *Pinctada margaritifera*: Structural and Biochemical Evidence for a Sequential Development of the Calcite Units

Jean-Pierre Cuif ^{1,*} , Angélique Fougereuse ², Cedrik Lo ² and Yannicke Dauphin ³ 

¹ Centre de Recherche sur la Paléodiversité et les Paléoenvironnements (CR2P), UMR 7207, Muséum National d'Histoire Naturelle, 75005 Paris, France

² Direction des Ressources Marines, BP 20, Papeete 98713, French Polynesia; angelique.fougereuse@administration.gov.pf (A.F.); cedrik.lo@administration.gov.pf (C.L.)

³ Institut de Systématique, Evolution, Biodiversité (ISYEB), UMR 7205 CNRS, Sorbonne Université, EPHE, Muséum National d'Histoire Naturelle, 75005 Paris, France; yannicke.dauphin@sorbonne-universite.fr

* Correspondence: jean-pierre.cuif@mnhn.fr

Abstract: Calcite prismatic units that form the outer layers of “nacro-prismatic” Pelecypod shells are often used as biomineralization models due to their individual size, simple shape, and spatial arrangement. However, these models do not take into account the developmental history of the shell. After metamorphosis, a series of structural changes predating production of the prisms is commonly missing. Consequently, this study focuses on the early stages of the calcite biomineralization area of the *Pinctada margaritifera* as it occurs in the outer mantle groove. It also includes the structural changes following the typical “simple prism” status. The interpretation takes advantage of an ancient result from genomic investigations: the localisation of Prsilkin-39, a protein associated with production of the calcite units. A revision of the initial interpretation concerning the position of this Prsilkin-39-producing area provides additional evidence of the role of two distinct mineralizing sectors in the formation of the calcite units in the *Pinctada* shell: the outer mantle groove and the anterior mineralizing area of the shell mantle.

Keywords: *Pinctada*; shell development; calcite prisms; Prsilkin-39



Citation: Cuif, J.-P.; Fougereuse, A.; Lo, C.; Dauphin, Y. Formation of the Outer Shell Layer in *Pinctada margaritifera*: Structural and Biochemical Evidence for a Sequential Development of the Calcite Units. *Minerals* **2023**, *13*, 1301. <https://doi.org/10.3390/min13101301>

Academic Editor: Alejandro B. Rodriguez-Navarro

Received: 13 September 2023

Revised: 1 October 2023

Accepted: 5 October 2023

Published: 8 October 2023



Copyright: © 2023 by the authors. Licensee MDPI, Basel, Switzerland. This article is an open access article distributed under the terms and conditions of the Creative Commons Attribution (CC BY) license (<https://creativecommons.org/licenses/by/4.0/>).

1. Introduction

Mollusk shells are natural biocomposites with a wide range of applications, including paleo-environmental records [1,2], phylogenetic reconstruction [3–5], and biomarkers for stratigraphy [6]. A reliable understanding of shell mineralization and growth is essential for many of these investigations. However, despite Mollusca being the second-largest phylum among invertebrates, detailed knowledge of shell growth is limited to only a few species. It seems that the larval shells of mollusks consistently feature aragonite and exhibit comparable, if not indistinguishable, structural patterns [7–10].

The *Pinctada* genus, which is known for its significant contribution to pearl production among Pelecypods, is frequently used as a microstructural model to study nacro-prismatic shells. In *P. margaritifera*, the species used for pearl production in Polynesia, the outer layer of the shells consists of calcite units, described as large polygonal prisms that are approximately 50 µm in transversal sections and up to 2 mm in length. These prisms are consistently oriented perpendicular to the shell surface, forming a thinner layer than the thick nacreous layer found on the inner side of the shell, in which the aragonite units are about 10 µm in the transversal dimension and 0.5 to 0.8 µm in thickness (Figure A1).

The periostracum, the third component of the shell, is often overlooked. Initially referred to as the epidermis and later named the periostraca [11], it was quickly recognized

for its protective function. Over time, the importance of this organ has become increasingly understood, as it has been acknowledged as a potential source of “discrete calcified structures” such as spicules and spikes [11].

The structural evolution of the calcite units between the shell metamorphosis and the adult stage of the *Pinctada margaritifera* shows that mineralization of its shell outer layer is actually more complex. The complexity involves a linear sequence of microstructural changes.

2. Major Steps in the Development of the Calcite Prism in the *Pinctada* Shell

2.1. The Post-Metamorphosis Mineralization

Embryonic and larval developments of *Pinctada margaritifera* were described and compared to those of *P. fucata* [12–16]. After a complex larval development whose final stage consists of a wholly aragonite shell with a granular microstructure (Figure 1a–c), the post-metamorphosis mineralization is characterized by the development of two structurally distinct layers. Formation of the outer layer does not change the shell profile (Figure 1d), but the shell surface is subdivided into distinct units (Figure 1e). Each unit exhibits precise limits and an individual centre (red arrows). Additionally these units are no longer made of granular aragonite but are built by calcite. Unexpectedly, upon examination of the growing surfaces of these newly formed structural units, it is evident that their fine-scale growth lines maintain the overall growth directions of the larval shell, with only weak inflexion marking the individuality of each structural unit (Figure 1f). Further analysis under transmitted polarized light confirms the distinctiveness of these polygonal units while also revealing their imperfect crystallization (Figure 1g). The polarisation colours vary irregularly within a given structural envelope.

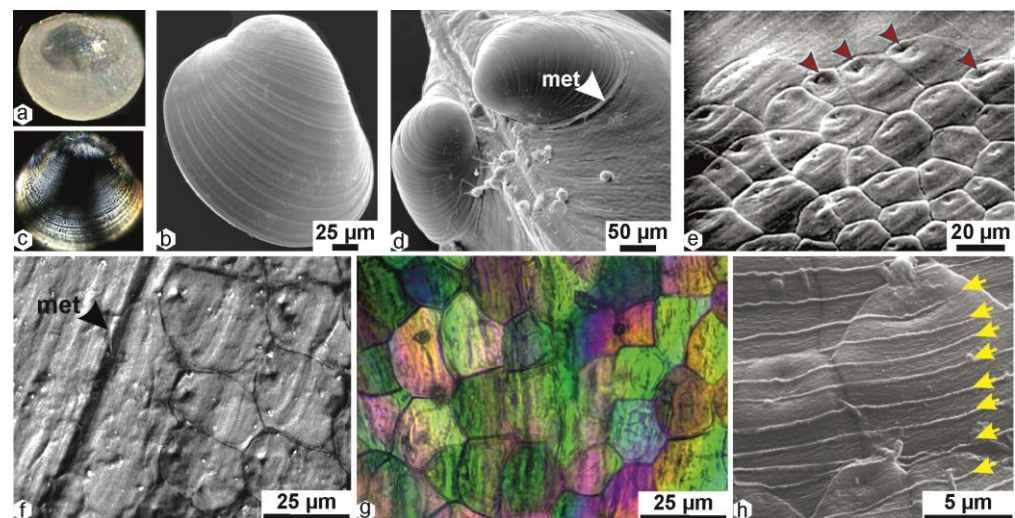


Figure 1. External view of the interface between the final larval shell and the first post-metamorphosis mineralization in the pearl oyster *Pinctada margaritifera*. (a) External morphology of a 6-day larval stage; full size 120 µm. (b) Overall morphology of the final larval stage, showing the regularity of the growth layers. (c) Final larval stage viewed under optical transmitted polarized light, revealing oriented aragonite particles creating a black crossed figure. (d) Trace line of the shell metamorphosis (met) showing the continuity of the shell growth profile between the larval and juvenile shells. (e) Occurrence of the first microstructural indication of metamorphosis. Note the polygonal limits and the centre of each polygonal unit, marked by red arrows. (f) Closer view of the growth lines of the calcite in the juvenile shell units. The overall growth direction is weakly changed; met: a morphological trace of the metamorphosis. (g) Crystallographic individuality of the calcite units in the juvenile shell. The variability of the polarisation colours within a given structural unit is explained by the specific local arrangement of the layers of calcite particles (see Figure 2). (h) Stepping growth mode of the periostracum; steps are marked by yellow arrows.

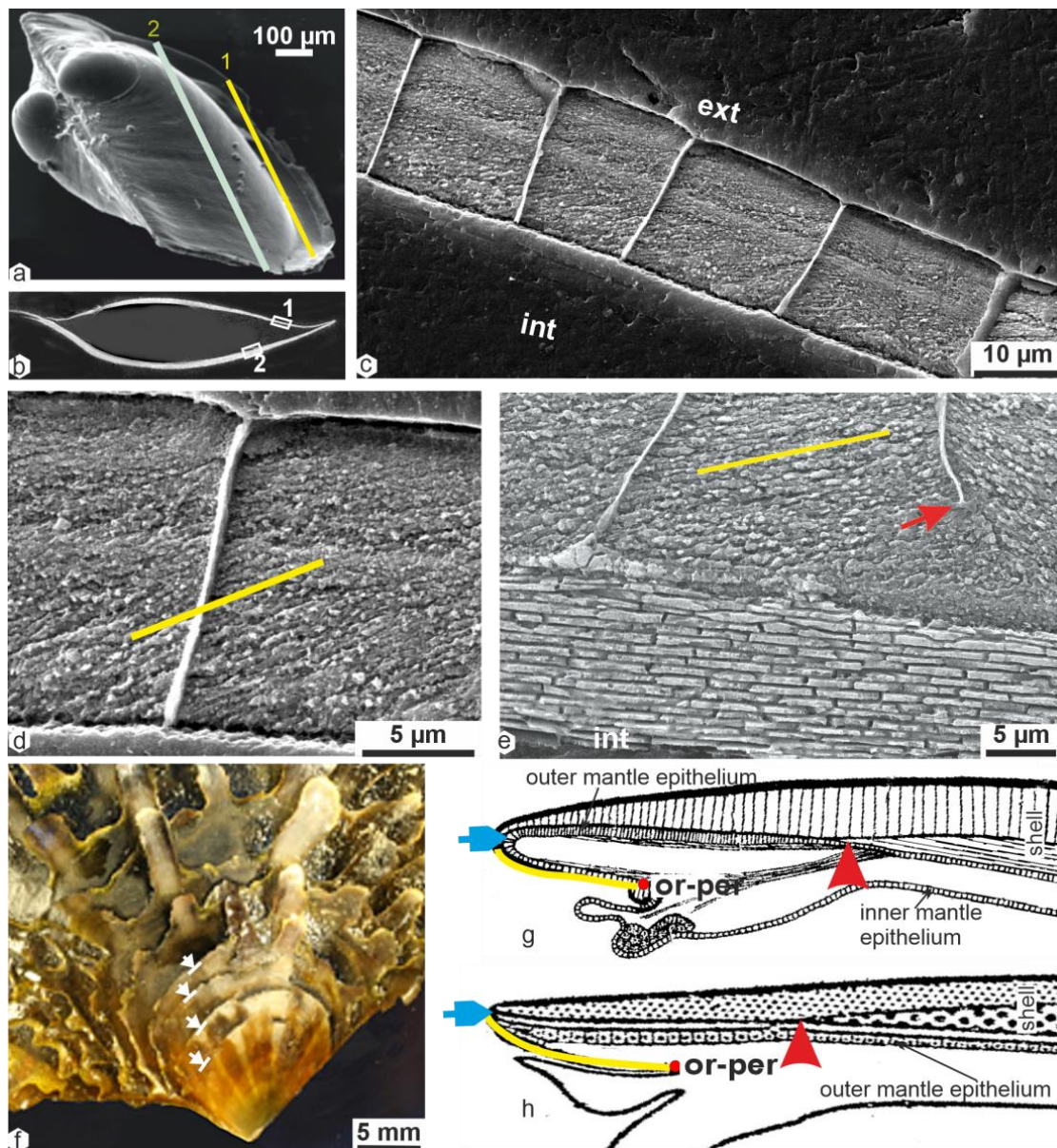


Figure 2. Shell microstructures in the prismatic and nacreous layers of juvenile *Pinctada margaritifera* shells. (a,b) Juvenile (post-metamorphosis) stages: external view (a); transversal sections (b). The sections are perpendicular to the growth direction of the shell: only the outer shell layer is shown in Section 1; both outer and inner shell layers are shown in Section 2. (c,d) Microstructure of the prismatic portion of the shell. The layers of mineral particles are oriented oblique with respect to shell surface (yellow lines) and not influenced by the prismatic boundaries. This accounts for the variation in colour of the prism sections viewed under transmitted polarized light (see (f)). (e) Nacreous layer showing the usual “brick and mortar” arrangement. Note the imperfection of the interprismatic membrane (red arrow) and the diverse orientations of the layers of calcite particles. The mineralization mechanism of the prisms is still imperfect. (f) Formation of growth scales (white arrows) on the external surface of the shell; this event marks the end of the juvenile stage. The overall organisation of the shell is now comparable to the anatomical schemes. (g,h) Overall organisation of the growing shell [17,18]. (h) Blue arrows indicate the contact points between the shell made of calcite disks grown in the outer mantle groove and the shell made of prisms by the outer layer of the mantle mineralizing area.

The periostracum, an additional structure on the outer surface of the shell, has a stepping growth mode (Figure 1h). This is evident from the continuity of the growth lines between neighbouring mineral units.

From its earliest origin, the outer layer of the shell has a prismatic structure. The boundaries of the prismatic units are generally perpendicular to the shell surface, but not perfectly so. The prismatic units are formed by superposed growth layers, which are not parallel to the inner surface of the shell. The growth layers consist of distinct mineral particles and have an overall oblique orientation with respect to growth direction. The yellow lines in Figure 2a,c,d show the orientation of each growth layer. In some cases, the growth layers extend from one prismatic unit to a neighbouring one through the prism membrane (Figure 2d). In other cases, as shown in Figure 2e, one of the prismatic units is not entirely isolated from its neighbour by an organic envelope.

The variable orientation of the transmitted-light polarisation colours in the given early post-metamorphosis prisms (Figure 1g) is an obvious consequence of the variable distribution of the growth surfaces in the given prismatic units.

This suggests that after the aragonite control of crystallization exerted on the granular growth layers of the larval shell (Figure 1b,c), the biochemical control over new calcite crystallization in the early prismatic units is not fully established in the early stages of the prismatic structures.

2.2. Microstructural Consequences of the Occurrence of Shell Scales

An important biological step in shell formation is illustrated in Figure 2f, where the first shell scale is visible. Unlike the previous phase, where the outer surface of larval and juvenile shells maintained a flat structure despite undergoing structural and mineralogical changes, a scaly growth mode of the shell becomes prevalent for the rest of the animal's life. It is noteworthy that this scaly growth mode implies that the end of a growth period is marked by the retraction of the animal mantle below the anterior portion of the newly mineralized shell surface. This event is particularly significant in relation to the periostracal membrane, which is disrupted by the retraction, with intensity of this process depending on circumstances. The section of the periostracum that retracts promptly adheres to the inner surface of the shell, irrespective of the mineral composition of the area, whether calcite or aragonite.

Throughout the animal's life, this process is repeated. When the mineralization process restarts, the stepping growth mode of the periostracum begins from the point of retraction. Figure 2g [17] and Figure 2h [18] provide an appropriate presentation of the anatomical organisation of a nacre-prismatic shell, adapted to the Japanese pearl oyster in the figure by Wada [18]. In both cases, we can see that the origin of the periostracum is not located at the shell growth edge but much further back, in the deeper part of the outer mantle groove. This location is of major interest because, in contrast to the common view, the organisation and structure of the calcite prisms are directly linked to the stepping mineralization process, which is active over such a long distance, between the origin of the periostracum and the shell growing edge. The specific mineralization process starting in this area reveals the new microstructural organisation of the *Pinctada* prismatic layer and how it differs from the initial post-metamorphosis prisms.

2.3. Calcification Associated with Periostracum Growth: Specific Mineralization Process Predating Prism Formation

The periostracum is produced by a dedicated group of cells located in the deeper part of the outer mantle groove (Figures 3a and A2). When the shell is actively growing, this thin membrane can serve as a substrate for the deposition of calcium carbonate by the inner cell layer of the outer mantle groove [19,20]. Figure 3 provides significant information about the physical characteristics of the mineralized units associated with the periostracum in *Pinctada*.

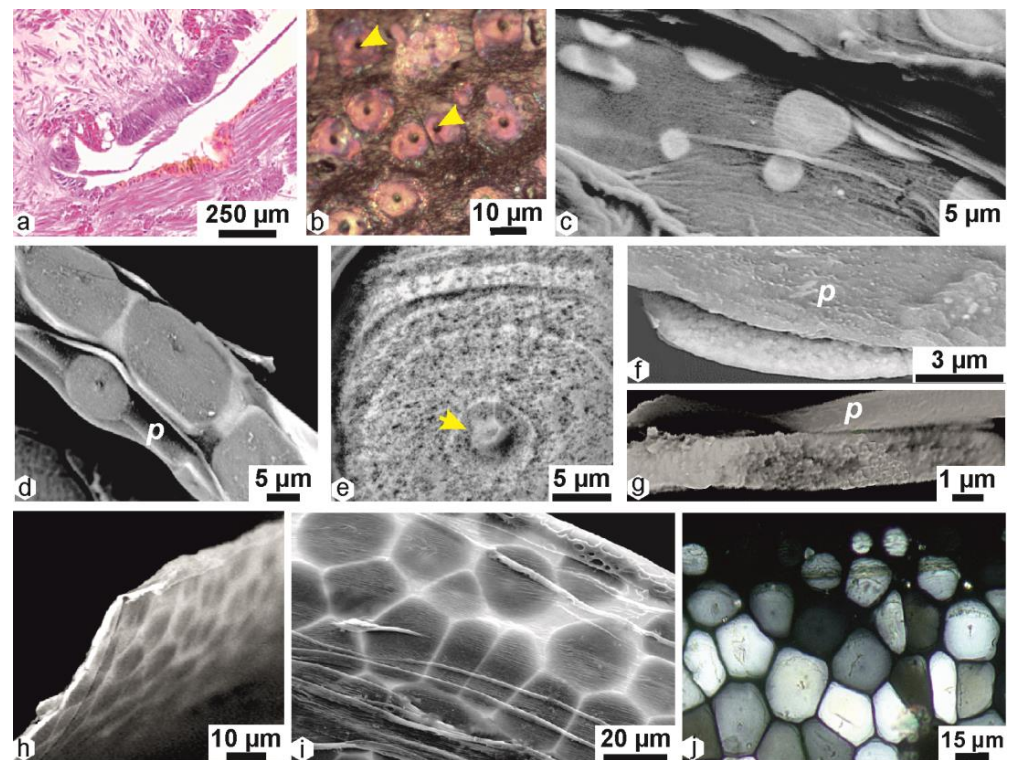


Figure 3. Development of calcite discoid units in the outer mantle groove of *Pinctada margaritifera*. (a) Histological section showing the origin of the periostracum in the deeper part of the outer-mantle groove (staining: Harris hematoxylin/eosine). (b) Earliest mineral deposition of the disks around the centres (yellow arrows). (c,d) Progressive development of the flat disks on the internal side of the periostracum (p). (e) Around their initial centre (yellow arrow), the disks grow by the concentric addition of calcite rings. (f,g) External view of a disk (partial view) on the internal side of the periostracum (f); same example of a fractured disk showing the absence of thickness increase (g). (h,i) Overall view of the “flexible shell” (h) internal side; (i) external side, covered with the disrupted part of the periostracal lamella. (j) The calcite units viewed in transmitted polarized light.

Located on the inner side of the periostracum, these calcite units are constructed around organic centres (Figure 3b, yellow arrows) by the repeated deposition of distinct but superimposed calcite rings (Figure 3c,e). The superposition of rings occurs in the same plane throughout the whole growth process associated with periostracum growth, resulting in a series of flat growing units approximately 3 μm in thickness (Figure 3f,g). Following the periostracum transit as schematised in the Wilbur or Wada schemes (Figure 2g,h), this series of individually distinct disks forms a sort of flexible shell on the inner side of the periostracum (Figure 3h,i). It is important to note that this flexible shell arriving at the shell growing edge is built by crystallographically distinct units, as shown by the various grey colours observed in transmitted polarisation light. Due to the high refractive index of calcite, this colour diversity in calcite units of similar thickness shows that they are differently oriented from a crystallographic standpoint (Figure 3h–j) [21]. The flexibility of the growth margin of the valves has been identified in Pterioidea, but the microstructure of this area has not been studied. These flexible margins allow a tight seal between the two valves [22].

2.4. Origin of the Prismatic Units at the Shell Grooving Edge: Transition between the Calcite Disks of the Flexible Shell and the Mantle-Secreted Calcite Prisms

The flexible shell expands outward as long as it remains within the outer mantle groove. When the calcite disks reach the end of the outer mantle groove, a critical ontogenetic process takes place: the calcareous units participate in the subsequent step of developing the prismatic outer shell layer. This is done through the backward movement of the

periostracum (Figure 2g,h). As a result, the neighbouring disks expose their internal side to direct contact with the mineralizing material generated by the mineralizing cell layer of the outer mantle.

Since the recognition of extracellular calcite crystallization during the growth of an echinid larva [23], the two-step mineralization of biogenic carbonate has become a widely accepted model. In this model, an intracellular concentration of amorphous calcium carbonate (ACC) occurs within the mineralizing cell layers, along with taxonomy-dependent organic components. This is followed by exocytosis and extracellular crystallization. Regarding the crystallographic properties of the *Pinctada* prisms, this scheme contributes to explaining their individual crystallization. The amorphous mineralizing material secreted by the mineralizing cells at the periphery of the mantle is produced against the distinct units produced by the outer mantle groove. Figure 4 summarizes the transitional process by which the circular units of the “flexible shell” are incorporated into new growth units produced at the periphery of the mantle mineralizing area.

It is important to note that shell growth does not occur continuously but in successive growth sequences, during which the sizes of the structural units repeatedly vary from smaller to larger diameters (Figure 4a–d). Figure 4e shows a fragment of the upper surface of a growing shell, on which a series of circular structures is visible. These concentric growth traces are clearly inherited from the previous disk development. However, we can see that new mineral material has been added between the circular structures inherited from the “flexible shell”, and a new polygonal framework (Figure 4e, red arrows) has been produced.

This inclusion process also occurs in more advanced structures of the flexible shell (Figure 4f). We can observe that each of the polygons built by the new polygonal network may include one or several of the morphologically irregular “disks” in a more regularly sized polygonal unit (Figure 4g). Optical microscopy of a part of Figure 4g shows the distinct difference between the irregularly circular envelopes of the “disks” and the polygonal envelopes produced by the mantle mineralization (yellow and red arrows).

As a result, the first new polygonal units are composite structures, built in part by components of the “flexible shell” and in part by new mineral deposits produced by the mineralizing mantle layer (Figure 4g). Through this crucial process, the transformation from a “flexible shell” to a rigid structure takes place.

Of particular importance from a microstructural viewpoint is the formation of new polygonal envelopes by the mantle mineralizing cells. These envelopes may include a variable number of the underlying circular disks of the “flexible shell”. This is typical for the contact layer between the end of the “flexible shell” secreted by the outer mantle groove and the first layer of the outer mantle epithelium (Figure 4f,g).

Figure 4h shows the interface between the new polygonal envelopes and the inner side of the periostracum (*per*). From this point, each of the subsequent secreted layers responsible for the elongation of a given prism will be built by a single crystal-like unit that will preserve the crystalline orientation of the underlying disk.

With respect to shell growth, it must be noted that the transitional mechanism is essential, as new disks consistently reach this pivotal stage in shell development. Therefore, the transitional stage simultaneously results in the shell’s thickening, achieved through prism elongation, and the lateral expansion of the “rigid shell” by integrating new growth units.

Optical observation of the shell microstructure immediately below the surface (Figure 4i) shows that the traces of the transitional process have disappeared. The different polarisation colours in neighbouring prisms (thin section = identical thickness for every section) indicate their distinct orientations.

The periostracum alteration on the profile view of a young shell growing edge (Figure 4j) reveals the traces of this transitional process, including the places of the disks on the upper surface and the adjunction of prism growth units that are synchronous on the entire mineralizing surface.

The single-crystal behaviour of each prism is confirmed by etching of a polished surface perpendicular to the prisms' elongation (Figure 4k), which shows the different crystalline orientations of each prismatic unit.

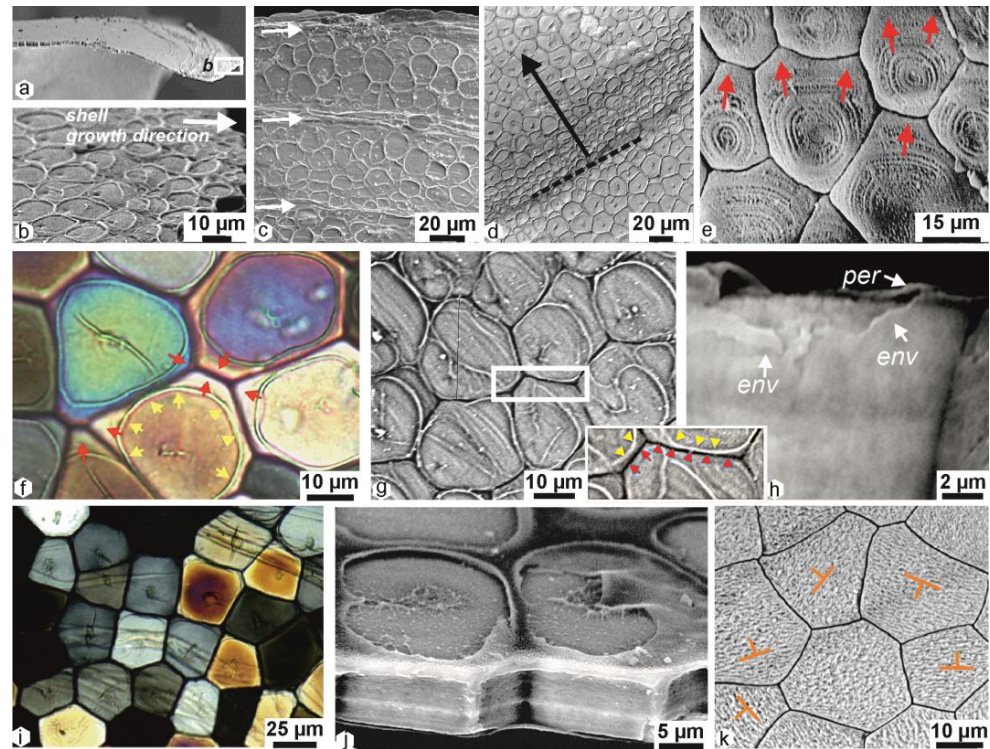


Figure 4. Contact between the disks of the “flexible shell” and the mineralizing secretion by the mantle at the shell growing edge of *Pinctada margaritifera*: transfer from disks to prism crystallization. (a,b) Outer view of the growing area in a young shell (a); the circular morphology of the majority of the disks (b). (c,d) Variation of the disk sizes during the growth sequences. The calcite units display repeated series of growing diameters separated by white arrows (c), making obvious a periodic growth mode, individually illustrated (d). (e) Example of prism growth in a very young prism growth stage: the mineral phase of the circular ovoid disks is supplemented by an additional deposition inside the polygonal envelopes. (f) Prism formation by disks that are more advanced in their development have visible envelopes (yellow arrows) and are also completed by additional calcite depositions (red arrows) inside the polygonal envelopes (optical transmitted polarized light). (g) Similar case viewed by SEM: note the difference in the electron backscattering signal from the disk envelopes (white) and polygonal envelopes (black), emphasizing the different chemical composition of the mineralizing limits; in the illustrated sector, disk envelopes are marked by yellow arrows and polygonal envelopes by red arrows. (h) Junction (dash line) between the periostracum (per) and the polygonal envelope, partly degraded in its upper part. (i) Very young prisms on the inner part of the growing shell; the process of transition from disks to prisms is now over, and each prism grows as a single-crystal unit. (j) Residual disks (heavily degraded) followed by synchronical layers produced by the mantle mineralizing layer. (k) Evidence of prisms as the single-crystal units revealed by acidic etching of the mineral phase; each prism exhibits its own specific crystal structure.

2.5. Structural Differentiation of the Prisms during Growth

The examination of longitudinal sections (perpendicular to the shell surface) immediately after their formation provides clear insights into the distinct growth pattern of the prisms. Perfect synchronisation in the formation of superimposed growth layers is readily evident upon close examination (Figure 5a,b). Various patterns of extinction within the prisms of *Pinctada* are described. After dissolution of the organic envelopes using oxidizing agents or enzymes, the mineral component of the prisms becomes visible (Figure 5c), show-

ing that this regular growth mode is maintained for several tens of micrometres [24–26]. Nevertheless, a small increase in the diameter of the young prisms suggests the disappearance of some of them. A more significant change occurs abruptly after approximately 100 to 150 μm of longitudinal growth (Figure 5d). This increase in diameter is correlated with a structural modification.

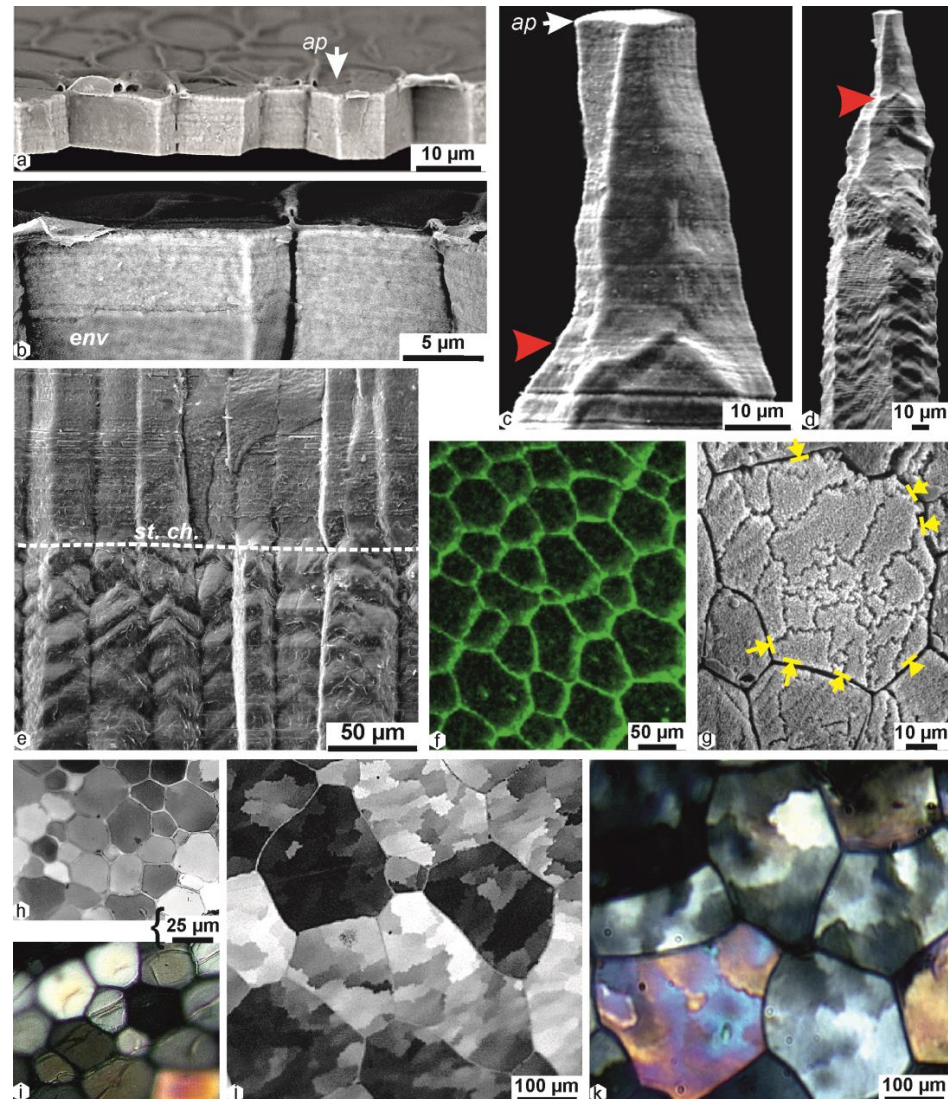


Figure 5. Morphological and structural changes during growth of the prisms in *Pinctada margaritifera*. (a,b) Initial growth stages of the polygonal prisms; the growth layers are now continuous between adjacent prisms, a synchronised process that differs from the individual growth mode of the disks. *ap*: apex of the prism; *env*: polygonal envelope of the prisms. (c,d) Morphological changes throughout prism growth. The low diameter increase in the initial growth stage (c) is followed by a rapid increase correlated to structural modification (d); (*ap*: apex of the prism). (e) The structural change (*st.ch.*) is a biologically driven process occurring synchronously between neighbouring prisms. The distinct single-crystal units (upper part of the picture) synchronically shift to oblique and complex crystalline units. (f) The large prisms surrounded by the UV fluorescence membrane. (g) Polished, fixed, and etched section showing the destroyed intraprismatic sinuous lacunae (yellow arrows); glutaraldehyde + formic acid + Alcian Blue solution. (h–k) Optical light microscopy of thin sections observed in epipolarisation (h–j) and transmitted polarized light (i–k). Both methods confirm the single crystalline status of the prisms in their initial growth stages (h,i) and their shift to a polycrystalline mineral structure during the rest of their growth.

Remarkably, the morphological and structural changes occur synchronously. In a given specimen, as shown in Figure 5e, the biomineralization of the prisms changes after an equivalent growth length as simple prismatic units. After this line of structural change (Figure 5e, *st.ch.*), control of mineral crystallization is reduced, as shown through the examination of polished surfaces or thin sections prepared perpendicular to the overall growth direction (Figure 5e–h).

3. Discussion: Biomineralization of *Pinctada* Prisms—Integrating Biological Data for Structural Analysis and Re-Examination of Former Models

The series of structural changes between the metamorphosis of the *Pinctada* larval shell and the complex polycrystalline units forming the main part of its adult outer shell layer lead to the conclusion that the concept of a “simple prism” is not appropriate for this species. A similar conclusion was reached when examining the structure and growth mode in the *Pinna* prism, another reference in structural classifications [27]. In both cases, biological control over calcification is shown to be dependent on progressively associated factors that govern the structural components. Many of these factors remain unknown, likely due to studies focusing on final structural stages and not identifying developmental stages. However, in the case of *Pinctada*, a calcite crystallization protein has been identified.

3.1. Prsilkin-39 Calcite-Producing Protein Is Limited to Initial Mineralization Area

The discovery of Prsilkin-39 was made in *Pinctada fucata* specimens collected from the Guofa Pearl Farm in Beihai, Guangxi Province, China [28]. This study reveals the identification of a novel molecule, Prsilkin-39, which shows a significant association with calcite production. Twelve co-authors employed a variety of biochemical methodologies to investigate the production of Prsilkin-39. Unlike studies that focus primarily on nacre, this research specifically focused on elucidating the biochemical control of calcite units in *Pinctada*, particularly the commonly referred to “prism” structure. The primary conclusion of the study is summarized in the final sentence of the abstract: “These observations have the potential to expand our understanding of the unique class of fundamental matrices and their roles in the development of molluscan shells”.

The authors of the study concluded that Prsilkin-39 likely serves two functions: it helps to build the organic framework of the calcite prismatic layer, and it inhibits the formation of aragonite crystals [28].

As depicted in Figure A2a (replicating Kong et al. [28], Figure 4a), the calcite associated with Prsilkin-39 is exclusively produced in the outer mantle groove of *Pinctada fucata* (Figure 2a: blue arrow). The point of maximum secretion intensity for Prsilkin-39 (indicated by three black arrows in Kong et al. [28], Figure 4a) precisely aligns with the region where the periostracal disks attain their largest sizes within the outer extrapallial groove, exhibiting maximal diameters and periostracum coverage (Figure 3 in this study). It is important to note that the discovery of calcite production through mineralization in the outer mantle groove emerged after 2009 and was not considered during the initial identification of Prsilkin-39. The Kong study concludes that Prsilkin-39 is associated with the calcite produced in the outer mantle groove [28].

So, the genomic expression region of Prsilkin-39 does not align with the formation of the calcite prisms, as indicated by the authors of the discovery. Instead, it corresponds to the mineralizing cells within the outer mantle groove, where the growth of calcite disks occurs.

This discovery significantly contributes to our comprehension of the distinction between the individual concentric crystallization process of calcite in the outer mantle groove and the calcite crystallization facilitated by the outer mineralization layer. The biochemical evidence reinforces the concept that the backward movement of the periostracum (Figure 1i,j) during the initial formation of scales corresponds to the emergence of a novel mineralization mechanism within the calcite mineralization region.

3.2. Former Interpretations of Prism Formation and Origin of the Prismatic Shell Layer in *Pinctada*

Initially, research on shells predominantly concentrated on mollusks that were readily accessible for collection. These mollusks were commonly found in freshwater environments, such as *Anodonta* and *Unio*, or in nearby seas, like *Pinna* [29–31]. Boggild did not detail the structure of the *Pinctada* shell [32]. Nevertheless, he did establish three distinct categories of prismatic structure: the “normal”, the “complex”, and the “composite” prismatic structure. Within the normal group, “each prism consists of a single crystallographical individuum unit. . .”. The complex prismatic structure is identified by the presence of an aggregation referred to as the “homogeneous one” (p. 15). The composite prismatic structure comprises larger prisms (prisms of the first order), each composed of fine prisms (the second order) arranged in a feathery manner.

Taylor et al. confirmed that Pteriomorphia shells are bilayered, with an outer calcite layer made up of polygonal columns that are perpendicular to the shell surface, and an inner nacreous layer [33,34]. They also confirmed “that each prism extinguishes in several smaller blocks”, as shown by Watabe and Wada [24]. Additionally, they assigned a major role to the periostracum, which acts as the substrate for the initial nucleation and crystal growth of the outer shell layer. This layer is secreted by the outer surface of the outer mantle fold.

Nakahara and Bevelander [35] conducted a study to investigate the growth mode and origin of the prisms in *Pinctada radiata*. Using transmission electron microscopy, they obtained detailed structural information after the decalcification process. Their study provided the first evidence of two distinct mineralized units that successively contribute to the development of the prismatic unit. One unit consists of flat structures that are consistently produced with a constant thickness. The other calcareous units exhibit an increasing thickness. Interestingly, the periostracum is involved in the interpretation of these “flat and thick” units (Figures 14 and 15) [35]. A synthetic scheme (Figure 16) [35] precisely describes the respective roles of these calcareous units in shell development. In Nakahara and Bevelander’s interpretation, these two distinct calcareous units are associated with the retraction of the animal within the shell. During this process, the periostracum adheres to the inner surface of the shell. When growth restarts, the periostracum first covers the formation of thin calcareous units, followed by thicker units that build more internal areas. Nakahara and Bevelander [35] explicitly state that the cells forming the flat and thick calcareous units are essentially similar from a mineralizing viewpoint. They say that “Detailed examination of the cells in different parts of the mantle shows, except for a difference in height, no cytological features that suggest a possible functional specialization regarding the formation of the various elements of the prism” (p. 43, Discussion). However, this statement is contradicted by the structural and biochemical evidence gathered in the previous pictures. The pictures show that the cells forming the flat units are much smaller than the cells forming the thick units. The flat units also have a different crystallographic orientation than the thick units. This suggests that the cells forming the flat units are specialized for producing a different type of mineral than the cells forming the thick units.

From a biological standpoint, the sequential arrangement of the two different calcareous units (the flat ones followed by the thicker or elongated ones) is clearly linked to the retraction of the animal, as shown by the interpretation in Figure 16D [35]. However, despite the morphological difference between the “flat” and “thick” units, the Nakahara and Bevelander model appears to be related to a single-step biomineralization process. There is no mention, in either the structural descriptions or the cytological data, of a distinct mineralization process for the thin and long prisms as they are now illustrated.

Checa et al. made meticulous observations of calcite prisms in “oysters”, comparing them to aragonitic prisms in *Unio* and *Neotrigonia* [36–40]. They showed the topographical relationships between the periostracum, mantle cells, and shells. They also described the inner structure and crystallography of the calcite prisms in two species of *Pinctada*. Based on these data, Checa et al. were able to demonstrate that the hypothesis of Ubukata [41] was not appropriate for *Pinctada* shells. They stated that for these genera, the polygonal shape of

the prisms was not the result of crystal selection by competition. Instead, they emphasized the role of the organic interprismatic membranes, stating that “it is the membranes, not the mineral prisms that control the pattern” [38]. Thermogravimetric analysis (TGA) appears to demonstrate that there is no significant difference in the amount of intracrystalline organic component of the calcite prisms of *Pinctada* and *Atrina* (a close relative of *Pinna*) when the organic interprismatic envelopes are destroyed [42]. Therefore, Checa et al. suggest the “intracrystalline content as directly responsible for the misorientations”. However, despite these similarities, the composition of the organic content of *Pinna* and *Pinctada* strongly differs [25,43–45]. The intracrystalline organic matrix of *Pinna* is rich in acidic sulphated polysaccharides, while that of *Pinctada* is rich in proteins. Moreover, the distribution of the intracrystalline organic matrix is homogeneous in *Atrina* but heterogeneous in *Pinctada*. Checa et al. [36–40] also depicted the growth process of shells from an amorphous calcium carbonate precursor, but they did not discuss its structural arrangement.

The most recent model is based on observations conducted on the shell of *Pinctada margaritifera* [46]. This model outlines the process of forming an initial disk preceding the prisms, achieved by the transformation of “a mixture of amorphous CaCO_3 and organics into calcite”. This transformation follows a radial progression, with the hypothesized mechanism driving centripetal crystallization that leads to the exclusion of organic components towards the edge of the disk. Through this process, the disk becomes predominantly crystalline, with the organic components expelled further outward.

The initial disks appear to form directly at the growing edge of the shell, without any preceding biological history. Subsequent prisms are also formed by this same process, with the primary distinction being the acquisition of a polygonal transverse section due to mutual contact. This transformation turns the disks into prisms, separated by membranes that accumulate organics at the inter-prismatic regions. The prismatic structure directly follows the initial crystallization process, which can be locally influenced by factors like “strain” and “tilts” in areas rich in organics. Notably, there is no mention of structural changes occurring in the subsequent series of mineralized layers.

4. Conclusions

Existing prism-formation models, which primarily rely on well-established prismatic structures, offer a limited perspective on prism development. A closer examination of the progressive construction of these shell-building units reveals a more nuanced view of prisms.

Studies of post-metamorphosis prism development in *Pinctada* shells have unveiled the complexity of calcite mineralization. They undergo a series of structural transformations as they transition from aragonite larval development to calcite prism formation. Even models acknowledging the presence of calcite disks prior to prismatic structures struggle to reconstruct the entire sequence of structural steps in post-metamorphosis shell formation.

To summarize, examination of calcite mineralization in *Pinctada* shells has revealed three distinct areas:

Post-larval domain: Here, calcite mineralization exhibits structural similarities to the larval mineralization mode, with well-defined calcite units and oblique calcite layers.

Discoid mineralization: Associated with the scaly structure of the shell, this area sees the specific mineralization of calcite disks by outer mantle groove cells.

Prismatic mineralization: This pivotal phase in prism formation transfers crystallographic properties from the disks to the mantle growth layer. Each prism in the common mineralization layer crystallizes based on the substrate provided by the underlying disks, transforming the flexible shell into a rigid one.

Existing prism-formation models, based on measurements of adult prisms’ physical or chemical patterns, fail to reconstruct the critical earlier stages where essential prism characteristics are established. Moreover, these models overlook the final developmental stage of prism formation.

The commonly accepted “self-replication” model of prism growth through the initial layer is merely a transient phase, swiftly succeeded by the subdivision of single crystal-like prisms into polycrystalline structures. This suggests that calcite prisms in *Pinctada* are not as regular, simple, or stable as previously assumed. Instead, they are variable and constructed through a meticulously controlled sequence of events across the entire calcite biomineralization area. A comparative analysis with another “simple prism” reference among Pteriomorphid Pelecypods, the *Pinna nobilis* prism, leads to similar conclusions, raising questions about the validity of the “simple prism” concept.

Author Contributions: Conceptualization, J.-P.C.; investigation, J.-P.C. and Y.D.; resources, data curation, C.L. and A.F.; writing—original draft preparation, J.-P.C. All authors have read and agreed to the published version of the manuscript.

Funding: This research received no external funding.

Data Availability Statement: Not applicable.

Conflicts of Interest: The authors declare no conflict of interest.

Appendix A

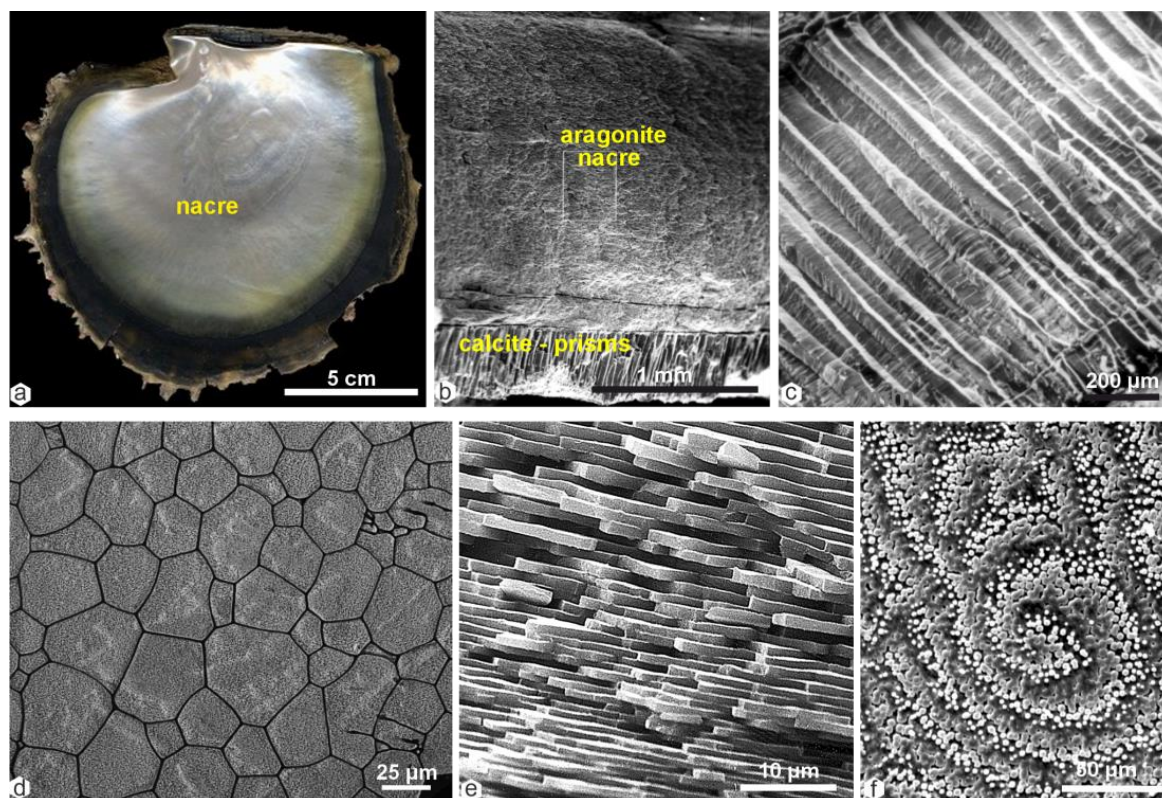


Figure A1. Structure of an adult *Pinctada margaritifera* shell. (a) Inner surface showing the nacre and the prismatic layers. (b) Fracture through the thickness of the shell, showing the thin outer prismatic calcite layer and the thick nacreous aragonite layer. Longitudinal (c) and transversal (d) sections in the prismatic layer. Longitudinal (e) and transversal (f) sections in the nacreous layer.

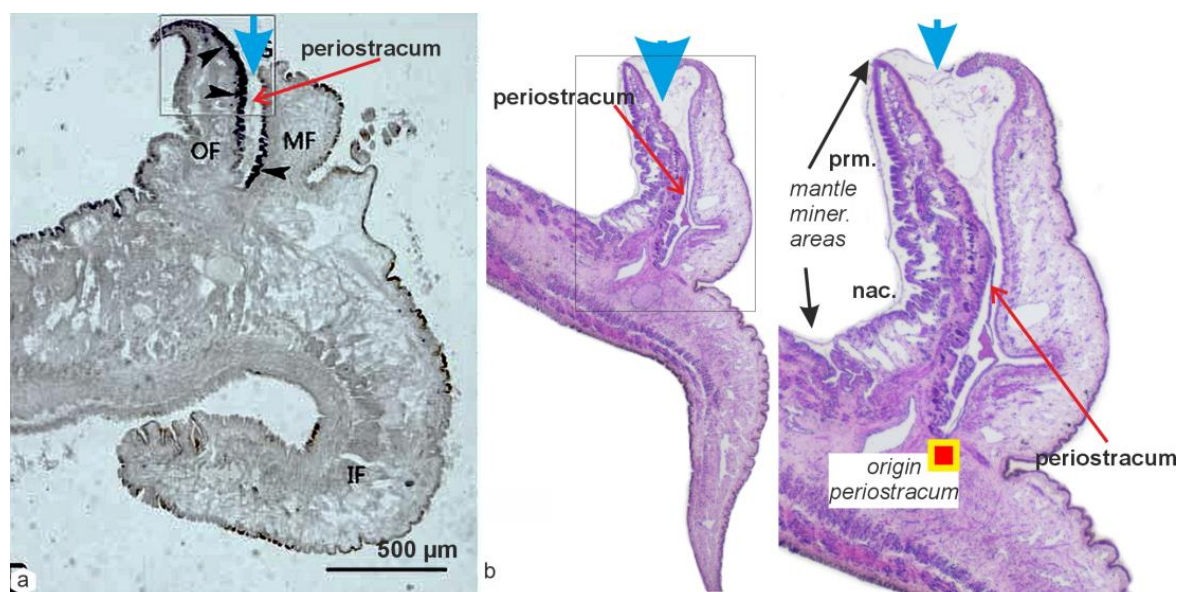


Figure A2. Comparison of the mantle structure of *P. fucata* and *P. margaritifera*. (a) Prislkin-39 is produced in the external mantle groove of *Pinctada fucata*, as denoted by the black arrows. This region is located between the OF and MF anatomical components, as identified by Kong et al. [28]. (b) Section of an equivalent area on a Polynesian *P. margaritifera*, stained with Harris's hematoxylin-eosin. Blue arrows indicate the Outer Mantle Grove entrance, and red arrows show the periostracum positions in both species.

References

- Mutvei, H.; Dunca, E.; Timm, H.; Slepukhina, T. Structure and growth rates of bivalve shells as indicators of environmental changes and pollution. *Bull. Inst. Océanogr. Monaco* **1996**, *14*, 65–72.
- Gröcke, D.R.; Gillikin, D.P. Advances in mollusc sclerochronology and sclerochemistry: Tools for understanding climate and environment. *Geo-Mar. Lett.* **2008**, *28*, 265–268. [[CrossRef](#)]
- Taylor, J.D. The structural evolution of the bivalve shell. *Palaeontology* **1973**, *16*, 519–534.
- Kobayashi, I. Various patterns of biomineralization and its phylogenetic significance in bivalve mollusks. In *The Mechanism of Biomineralization in Animals and Plants*; Omori, M., Watabe, N., Eds.; Tokai University Press: Tokyo, Japan, 1980; pp. 145–155.
- Kobayashi, I. Evolutionary trends of shell microstructure in Bivalve Molluscs. In *Mechanisms and Phylogeny of Mineralization in Biological Systems*; Suga, S., Nakahara, H., Eds.; Springer: Tokyo, Japan, 1991; pp. 415–419. [[CrossRef](#)]
- D'Orbigny, A. *Paléontologie Française: Description Zoologique Et Géologique de tous les Animaux Mollusques et Rayonnés Fossiles de France: Comprenant leur Application à la Reconnaissance des Couches*; Chez L'auteur: Paris, France; pp. 1842–1860, 4000p, 1440 pl.
- Stenzel, H.B. Oysters: Composition of the larval shell. *Science* **1964**, *145*, 155–156. [[CrossRef](#)] [[PubMed](#)]
- Carriker, M.R.; Palmer, R.E. Ultrastructural morphogenesis of prodissoconch and early dissoconch valves of the oyster *Crassostrea virginica*. *Proc. Natl. Shellfish. Assoc.* **1979**, *69*, 103–128.
- Eyster, L.S. Shell inorganic composition and onset of shell mineralization during Bivalve and Gastropod embryogenesis. *Biol. Bull.* **1986**, *170*, 211–231. [[CrossRef](#)]
- Weiss, I.M.; Tuross, N.; Addadi, L.; Weiner, S. Mollusc larval shell formation: Amorphous calcium carbonate is a precursor phase for aragonite. *J. Exper. Zool.* **2002**, *293*, 478–491. [[CrossRef](#)]
- Gray, J.E. Conchological observations, being an attempt to fix the study of conchology on a firm basis. *Zool. J. Lond.* **1825**, *1*, 204–223.
- Kobayashi, I. Shell structure of *Pinctada fucata martensii* (Dunker) in the larval and juvenile stages. *Earth Sci.* **1981**, *35*, 245–252. (In Japanese with English Abstract)
- Alagarwami, K.; Dharmara, J.A.; Chellam, A.; Velayudhan, T.S. Larval and juvenile rearing of black-lip pearl oyster, *Pinctada margaritifera* (Linnaeus). *Aquaculture* **1989**, *76*, 43–56. [[CrossRef](#)]
- Mao Che, L.; Golubic, S.; Le Campion-Alsumard, T.; Payri, C. Developmental aspects of biomineralization in the Polynesian pearl oyster *Pinctada margaritifera* var. *cumingii*. *Oceanol. Acta* **2000**, *24*, S37–S49. [[CrossRef](#)]
- Doroudi, M.S.; Southgate, P.C. Embryonic and larval development of *Pinctada margaritifera* (Linnaeus, 1758). *Moll. Res.* **2003**, *23*, 101–107. [[CrossRef](#)]
- Yokoo, N.; Suzuki, M.; Saruwatari, K.; Aoki, H.; Watanabe, K.; Nagasawa, H.; Kogure, K. Microstructures of the larval shell of a pearl oyster, *Pinctada fucata*, investigated by FIB-TEM technique. *Am. Miner.* **2011**, *96*, 1020–1027. [[CrossRef](#)]
- Wilbur, K.M. Shell formation and regeneration. In *Physiology of Mollusca*; Wilbur, K.M., Yonge, C.M., Eds.; Academic Press: New York, NY, USA; London, UK, 1964; Volume 1, pp. 243–282.

18. Wada, K. Biomineralogy and Pearl Culture—3. *J. Gemmol. Soc. Jpn.* **1975**, *2*, 99–104. [[CrossRef](#)]
19. Saleuddin, A.S.M. Shell formation in molluscs with special reference to periostracum formation and regeneration. In *Pathways in Malacology*; Van der Spoel, S., Van Bruggen, A.C., Lever, J., Eds.; Bohn, Scheltema & Holkema: Utrecht, The Netherlands, 1979; pp. 47–81.
20. Haas, W. Evolution of calcareous hardparts in primitive molluscs. *Malacologia* **1981**, *21*, 403–418.
21. Cuif, J.P.; Burghammer, M.; Chamard, V.; Dauphin, Y.; Godard, P.; Le Moullac, G.; Nehrke, G.; Perez-Huerta, A. Evidence of a biological control over origin, growth and end of the calcite prisms in the shells of *Pinctada margaritifera* (Pelecypod, Pterioidea). *Minerals* **2014**, *4*, 815–834. [[CrossRef](#)]
22. Harper, E.M.; Checa, A.G. Tightly shut: Flexible valve margins and microstructural asymmetry in pterioid bivalves. *Mar. Bio.* **2020**, *167*, 78. [[CrossRef](#)]
23. Beniash, E.; Aizenberg, J.; Addadi, L.; Weiner, S. Amorphous calcium carbonate transforms into calcite during sea urchin larval spicule growth. *Proc. R. Soc. Lond.* **1997**, *B264*, 461–465. [[CrossRef](#)]
24. Watabe, N.; Wada, K. On the shell structures of Japanese pearl oyster, *Pinctada martensii* (Dunker). (I) Prismatic layer. *Rep. Fac. Fish. Prefec. Univ. Mie* **1956**, *2*, 227–231.
25. Dauphin, Y.; Cuif, J.P.; Doucet, J.; Salomé, M.; Susini, J.; Williams, C.T. In situ chemical speciation of sulfur in calcitic biominerals and the simple prism concept. *J. Struct. Biol.* **2003**, *142*, 272–280. [[CrossRef](#)]
26. Dauphin, Y.; Zolotoyabko, E.; Berner, A.; Lakin, E.; Rollion-Bard, C.; Cuif, J.P.; Fratzi, P. Breaking the long-standing morphological paradigm: Individual prisms in the pearl oyster shell grow perpendicular to the *c*-axis of calcite. *J. Struct. Biol.* **2019**, *205*, 121–132. [[CrossRef](#)] [[PubMed](#)]
27. Cuif, J.P.; Belhadji, O.; Borensztajn, S.; Geze, M.; Trigos-Santos, S.; Prado, P.; Dauphin, Y. Prism substructures in the shell of *Pinna nobilis* (Linnaeus, 1758) Mollusca—Evidence for a three-dimensional pulsed-growth model. *Heliyon* **2020**, *6*, e04513. [[CrossRef](#)] [[PubMed](#)]
28. Kong, Y.; Jing, G.; Yan, Z.; Li, C.; Gong, N.; Zhu, F.; Li, D.; Zhang, Y.; Zheng, G.; Wang, H.; et al. Cloning and characterization of Prsilkin-39, a novel matrix protein serving a dual role in the prismatic layer formation from the oyster *Pinctada fucata*. *J. Biol. Chem.* **2009**, *284*, 10841–10854. [[CrossRef](#)]
29. Carpenter, W.B. On the microscopic structure of shells: Part I. *Br. Assoc. Adv. Sci.* **1844**, *14*, 1–24.
30. Carpenter, W.B. On the microscopic structure of shells: Part II. *Br. Assoc. Adv. Sci.* **1847**, *17*, 93–134.
31. Schmidt, W.J. *Die Bausteine des Tierkörpers in Polarisiertem Lichte*; Cohen, F.: Bonn, Germany, 1924; 528p.
32. Boggild, O.B. The shell structure of the molluscs. *D. Kgl. Danske Vidensk. Selsk. Skr. Naturvidensk. Ogmæthem.* **1930**, *9*, 231–326.
33. Taylor, J.D.; Kennedy, W.J.; Hall, A. The shell structure and mineralogy of the Bivalvia. I. Introduction. Nuculacea—Trigonacea. *Bull. Br. Mus. Nat. Hist. Zool.* **1969**, *3*, 1–125.
34. Taylor, J.D.; Kennedy, W.J.; Hall, A. The shell structure and mineralogy of the Bivalvia. II. Lucinacea-Clavagellacea. Conclusions. *Bull. Br. Mus. Nat. Hist. Zool.* **1973**, *22*, 253–294. [[CrossRef](#)]
35. Nakahara, H.; Bevelander, G. The formation and growth of the prismatic layer of *Pinctada radiata*. *Calcif. Tissue Res.* **1971**, *7*, 31–45. [[CrossRef](#)]
36. Checa, A.G.; Rodriguez-Navarro, A.B.; Esteban-Delgado, F.J. The nature and formation of calcitic columnar prismatic shell layers in pteriomorphian bivalves. *Biomaterials* **2005**, *26*, 6404–6414. [[CrossRef](#)]
37. Checa, A.G.; Bonarski, J.T.; Willinger, M.G.; Faryna, M.; Berent, K.; Kania, B.; Gonzalez-Segura, A.; Pina, C.M.; Pospiech, J.; Morawiec, A. Crystallographic orientation in homogeneity and crystal splitting in biogenic calcite. *J. Roy. Soc. Interface* **2013**, *10*, 20130425. [[CrossRef](#)] [[PubMed](#)]
38. Checa, A.; Macias-Sanchez, E.; Harper, E.M.; Cartwright, J.H.E. Organic membranes determine the pattern of the columnar prismatic layer of mollusc shells. *Proc. R. Soc.* **2016**, *B283*, 20160032. [[CrossRef](#)] [[PubMed](#)]
39. Checa, A.; Salas, C. Periostracum and shell formation in the Bivalvia. In *Treatise on Line*, 93; part N, revised; University of Kansas, Paleontological Institute: Lawrence, KS, USA, 2017; Volume 1, Chapter 3; pp. 1–51.
40. Checa, A.G. Physical and biological determinants of the fabrication of molluscan shell microstructures. *Front. Mar. Sci.* **2018**, *5*, 353.
41. Ubukata, T. Architectural constraints of the morphogenesis of prismatic structure in Bivalvia. *Palaeontology* **1994**, *37*, 241–261.
42. Okumura, T.; Suzuki, M.; Nagasawa, H.; Kogure, T. Microstructural variation of biogenic calcite with intracrystalline organic macromolecules. *Cryst. Growth Des.* **2011**, *12*, 224–230. [[CrossRef](#)]
43. Okumura, T.; Suzuki, M.; Nagasawa, H.; Kogure, T. Microstructural control of calcite via incorporation of intracrystalline organic molecules in shells. *J. Cryst. Growth* **2013**, *381*, 114–120. [[CrossRef](#)]
44. Suzuki, M.; Okumura, T.; Nagasawa, H.; Kogure, T. Localization of intracrystalline organic macromolecules in mollusk shells. *J. Cryst. Growth* **2011**, *337*, 24–29. [[CrossRef](#)]
45. Dauphin, Y. Soluble organic matrices of the calcitic prismatic shell layers of two pteriomorphid Bivalves: *Pinna nobilis* and *Pinctada margaritifera*. *J. Biol. Chem.* **2003**, *278*, 15168–15177. [[CrossRef](#)]
46. Duboisset, J.; Ferrand, P.; Baroni, A.; Grünewald, T.; Dicko, H.; Grauby, O.; Vidal-Dupio, J.; Saulnier, D.; Le Moullac, G.; Rosenthal, M.; et al. Amorphous-to-crystal transition in the layer-by-layer growth of bivalve shell prism. *Acta Biomater.* **2022**, *142*, 194–207. [[CrossRef](#)]

Disclaimer/Publisher’s Note: The statements, opinions and data contained in all publications are solely those of the individual author(s) and contributor(s) and not of MDPI and/or the editor(s). MDPI and/or the editor(s) disclaim responsibility for any injury to people or property resulting from any ideas, methods, instructions or products referred to in the content.